Received: 9 October 2019 | Revised: 17 December 2019 | Accepted: 18 December 2019

DOI: 10.1002/aoc.5469



Applied Organometallic Chemistry WILEY

FULL PAPER

# Nicotinic acid-supported cobalt ferrite-catalyzed one-pot synthesis of substituted chromeno[3,4-*b*]quinolines

**Mahdiye Foroughi Kaldareh** | **Masoud Mokhtary** | **Mohammad Nikpassand**

Department of Chemistry, Rasht Branch, Islamic Azad University, Rasht, Iran

**Correspondence**
Masoud Mokhtary, Department of Chemistry, Rasht Branch, Islamic Azad University, Rasht, P.O. Box 3516-41335, Iran.
Email: mmokhtary@iaurasht.ac.ir

One-pot synthesis of substituted chromeno[3,4-*b*]quinoline derivatives was developed by three-component reaction of aldehydes, dimedone or 1,3-cyclohexadione, and 4-aminocoumarin in the presence of nicotinic acid-supported cobalt ferrite [$CoFe_2O_4$@$SiO_2$@$Si(CH_2)_3Cl$@NA] as a novel magnetic catalyst in chloroform at reflux conditions. Nicotinic acid-supported cobalt ferrite was characterized via Fourier transform infrared spectroscopy, X-ray diffraction, thermal gravimetric analysis, scanning electron microscopy, high-resolution transmission electron microscopy, energy-dispersive X-ray spectroscopy, and vibrating sample magnetometry. Moreover, the catalyst could be easily recovered by magnetic separation and recycled up to five times without significant loss of its catalytic activity. The products formed in excellent yields over appropriate reaction times under environmentally friendly conditions. High efficiency and easy isolation of the catalyst from products by simple magnetic attraction are some of the considerable advantages of this procedure.

**KEYWORDS**

4-aminocoumarin, chromeno[3,4-*b*]quinoline, cobalt ferrite, nanocatalyst, one-pot synthesis

## 1 | INTRODUCTION

The development of magnetic nanoparticles (MNPs) for use as supports and exploration of their applications as catalyst in organic synthesis is an important green method as it is environmentally friendly and allows sustainable separation. By enabling simple recovery of MNPs from reaction media, different protocols involving surface modification, binding, and self-assembly offer a broad scope of approaches for preparing magnetically retrievable nanoparticles.[1] In recent years, the design and synthesis of nanomaterials with improved catalytic properties for use in photocatalysis and alcohol oxidation have been developed.[2–13] Cobalt ferrite nanoparticles have attracted continuous interest because of their unique properties and exceptionally promising applications. Cobalt ferrite has been utilized in various applications, such as magneto-optical devices,[14] magnetic hyperthermia,[15] and as contrast agent for magnetic resonance imaging.[16] Aminocoumarin derivatives have a wide range of biological applications,[17,18] such as antibiotics,[19] fluorescent markers,[20] melanin-concentrating hormone receptor antagonist,[21] inducing estrogenic activity,[22] carbonic anhydrase class of inhibitors,[23] and α-glucosidase inhibitors.[24] Organic compounds containing 4-aminocoumarin scaffold are synthesized by the reaction of 4-hydroxycoumarin, ammonia solution, Meldrum's acid, and aromatic aldehydes in the presence of SBA-15-$SO_3H$[25]; three-component reaction of 4-aminocoumarin, arylglyoxal monohydrates, and aromatic amines promoted by $KHSO_4$ in toluene under reflux condition[26]; three-component condensation of 4-aminocoumarin, aldehydes, and ethyl benzoylacetates

  

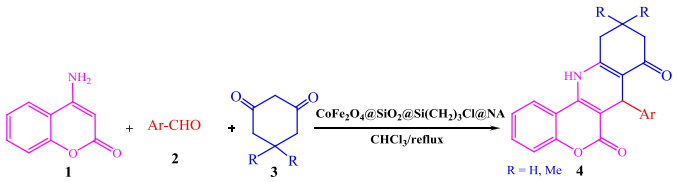


**SCHEME 1** Synthesis of chromeno[3,4-*b*]quinoline derivatives

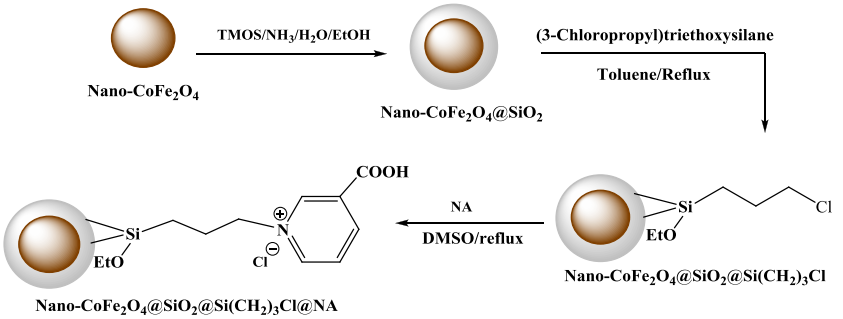


**SCHEME 2** Procedure for the synthesis of $CoFe_2O_4@SiO_2@Si\text{-}(CH_2)_3Cl@NA$ nanocatalyst. DMSO, dimethyl sulfoxide; TMOS, tetramethyl orthosilicate

by $POCl_3$ in dichloroethane under reflux conditions[27]; three-component domino condensation of 4-aminocoumarins, arylglyoxal monohydrates, and various nucleophilic substrates, such as arylamines, malononitrile, ethyl cyanoacetate, and cyanoacetamide-produced functionalized chromeno[4,3-*b*]pyrrol-4(1*H*)-ones in the presence of $Fe_3O_4@SiO_2\text{-}SO_3H$ nanoparticles as a solid acid catalyst under solvent-free conditions[28]; oxidative aromatization of tetrahydrochromeno[4,3-*b*]quinoline derivatives by nitric acid at ambient temperature[29]; two-component coupling of 4-aminocoumarin and α,β-unsaturated nitroalkene catalyzed by $PEG\text{–}SO_3H$[30]; three-component reaction of phenyl glyoxal, dimedone, and 4-amino coumarin to afford disubstituted chromeno[4,3-*b*]pyrrole-4(1*H*)-one derivatives catalyzed by $I_2$/dimethyl sulfoxide (DMSO)[31]; synthesis of coumarin fused to highly decorated indenodihydropyridyl and dihydropyridyl derivatives in the presence of (±)lactic acid/ethyl-L-lactate at 100 °C[32]; and synthesis of chromeno[4,3-*b*]quinoline derivatives in the presence of catalytic amounts of Cu(II)–Schiff base/SBA-15 by condensation of arylaldehydes with 1,3-cyclohexadione and then treating the obtained intermediates with 4-aminocoumarin in an autoclave at 200 °C.[33] Despite the potential utility of these methods, some suffer from disadvantages such as long reaction times, low yields, high reaction temperature, and the use of more corrosive catalyst. Because of the significance of chromeno[3,4-*b*]quinoline derivatives in pharmaceutical industries, there exists a need to develop effective, one-pot, and affordable procedures for the synthesis of these compounds. Following our interest in the use of magnetically separable catalyst in organic synthesis,[34,35] we herein report an efficient method for the synthesis of chromeno[3,4-*b*]quinoline derivatives by the reaction of aldehydes, dimedone or 1,3-cyclohexadione, and 4-aminocoumarin in the presence of nicotinic acid-supported cobalt ferrite [$CoFe_2O_4@SiO_2@Si(CH_2)_3Cl@NA$] as a novel nanocatalyst in chloroform at reflux conditions (Scheme 1). To the best of our knowledge, the $CoFe_2O_4@SiO_2@Si(CH_2)_3Cl@NA$ nanocatalyst has so far not been addressed in the relevant literature.

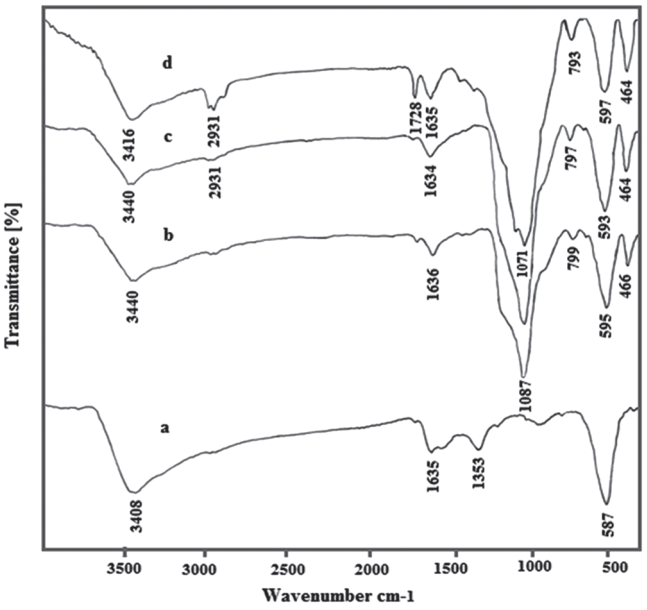


**FIGURE 1** Fourier-transform infrared spectra: (a) $CoFe_2O_4$, (b) $CoFe_2O_4@SiO_2$, (c) $CoFe_2O_4@SiO_2@Si\text{-}(CH_2)_3Cl$, and (d) $CoFe_2O_4@SiO_2@Si\text{-}(CH_2)_3Cl@NA$

## 2 | EXPERIMENTAL

### 2.1 | Material and methods

All chemicals were purchased from Merck Chemical Company, Darmstadt, Germany. Melting points (MPs) were recorded on an electrothermal MP apparatus. The nuclear magnetic resonance (NMR) spectra were recorded in DMSO-$d_6$ with TMS as the internal standard on a Bruker Avance DRX 300-MHz spectrometer. Fourier-transform infrared (FT-IR) spectra were determined on an SP-1100, P-UV-Com instrument. The saturation magnetization was deduced based on the hysteresis loop using a vibrating sample magnetometer (Meghnatis Kavir Kashan Co., Kashan, Iran). The energy-dispersive X-ray spectroscopy (EDS) analysis of the fabricated nanocatalyst was performed using a Philips XL30 microscope with an accelerating voltage of 20 kV. The field emission scanning electron microscopy (FESEM) image was obtained on a MIRA3 operated at an accelerating voltage of 15 kV. Prior to FESEM and EDS studies, each sample was gold sputtered. High-resolution transmission electron microscopy (HRTEM) images were obtained on an FEI (TEC9G20) operated at an accelerating voltage of 200 kV. The crystalline structure of the materials was evaluated using a diffractometer (Philips) with Cu-Kα radiation (λ = 1.54 Å). The thermal stability was determined by thermogravimetric analysis (TGA; Mettler Toledo) at a heating rate of 10 °C/min from room temperature to 600 °C in an inert atmosphere. Products were separated by simple filtration and identified by FT-IR, $^1$H NMR, $^{13}$C NMR spectra, and elemental analysis.

### 2.2 | Synthesis of $CoFe_2O_4$ nanoparticles

First, $FeCl_3{\cdot}6H_2O$ (6.5 g) and $CoCl_2{\cdot}4H_2O$ (2.85 g) were dissolved in distilled water (120 mL). After complete dissolution of the salts, NaOH (14.4 g) was dissolved in distilled water (120 mL) and added to the solution. The resulting black solution was vigorously stirred for 2 hr at 80 °C under $N_2$ atmosphere. The precipitated cobalt ferrite was then separated from the solution using a magnet and washed several times with distilled water. Finally, a stable black magnetic dispersion was obtained that was dried in an oven.

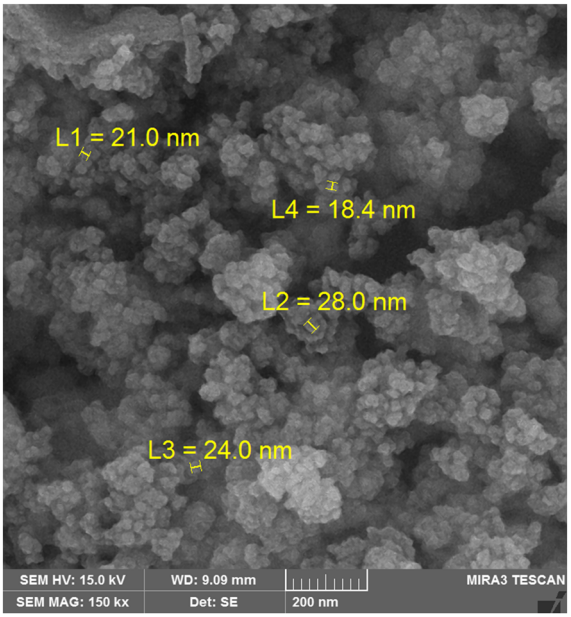


**FIGURE 3** Scanning electron microscopy image of the $CoFe_2O_4$@$SiO_2$@Si-$(CH_2)_3$Cl@NA nanocatalyst

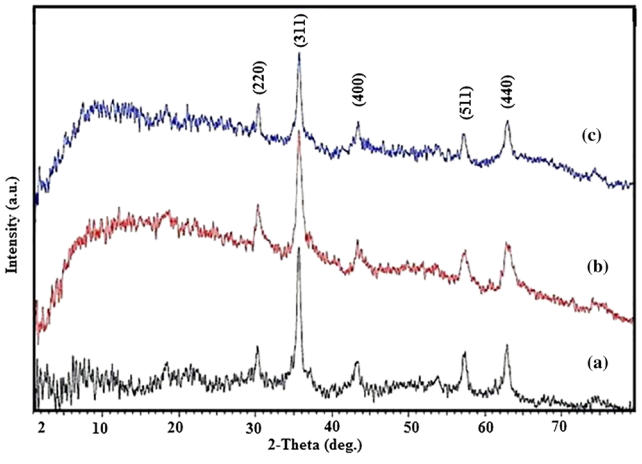


**FIGURE 2** X-ray diffraction patterns: (a) $CoFe_2O_4$@$SiO_2$, (b) $CoFe_2O_4$@$SiO_2$@Si-$(CH_2)_3$Cl, and (c) $CoFe_2O_4$@$SiO_2$@Si-$(CH_2)_3$Cl@NA

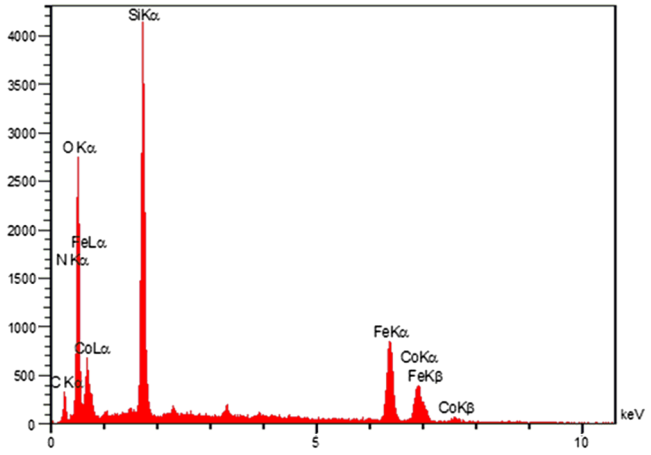


**FIGURE 4** Energy-dispersive X-ray spectroscopy spectrum of the $CoFe_2O_4$@$SiO_2$@Si-$(CH_2)_3$Cl@NA nanocatalyst

### 2.3 | Synthesis of $CoFe_2O_4@SiO_2$ nanoparticles

First, $CoFe_2O_4$ (1 g) nanoparticles were dispersed in a distilled water and ethanol mixture (80:20 v/v%) using ultrasound bath (15 min). Then, ammonia (2 mL, 28 wt%) and tetramethyl orthosilicate (2 mL) were added dropwise to the mixture which was stirred at 50 °C for 2 hr. The obtained $CoFe_2O_4@SiO_2$ nanoparticles were isolated using a magnet and then washed with distilled water and ethanol, respectively, and dried in an oven.

### 2.4 | Synthesis of $CoFe_2O_4@SiO_2@Si-(CH_2)_3Cl$ nanoparticles

First, $CoFe_2O_4@SiO_2$ (1 g) nanoparticles were dispersed in toluene (50 mL) by ultrasound bath (15 min). After that, (3-chloropropyl)triethoxysilane (2 mL) was gently added to the mixture and refluxed at 110 °C for 24 hr. The synthesized nanoparticles were separated using a magnet, washed several times with toluene and water, respectively, and finally the product was dried in an oven.

### 2.5 | Synthesis of $Fe_3O_4@SiO_2@Si-(CH_2)_3Cl@NA$ nanocatalyst

Nicotinic acid (1.5 g) was dissolved in DMSO (70 mL). Then, $CoFe_2O_4@SiO_2@Si-(CH_2)_3Cl$ (1 g) nanoparticles were added to the mixture and dispersed by ultrasound bath (15 min). The mixture was then refluxed for 24 hr. Finally, $CoFe_2O_4@SiO_2@Si-(CH_2)_3Cl@NA$ nanoparticles were separated using a magnet and washed with DMSO (50 mL) and dried in an oven.

### 2.6 | General procedure for the synthesis of chromeno[3,4-*b*]quinoline derivatives

A mixture of aldehyde (1 mmol), 4-aminocoumarin (2 mmol), dimedone or 1,3-cyclohexadione, and $Fe_3O_4@SiO_2@Si-(CH_2)_3Cl@NA$ (0.02 g) was dissolved in $CHCl_3$ (5 mL) and heated under reflux conditions. The progress of the reaction was monitored by thin-layer chromatography (ethyl acetate/*n*-hexane/methanol, 4:6:1). Upon completion of the reaction, the catalyst was separated using an external magnet and the crude product was recrystallized from ethanol (10 mL) to obtain the pure chromeno[3,4-*b*]quinoline derivatives.

## 3 | RESULTS AND DISCUSSION

### 3.1 | Characterization of the catalyst

In this study, nicotinic acid-supported cobalt ferrite [$CoFe_2O_4@SiO_2@Si(CH_2)_3Cl@NA$] as a novel magnetic

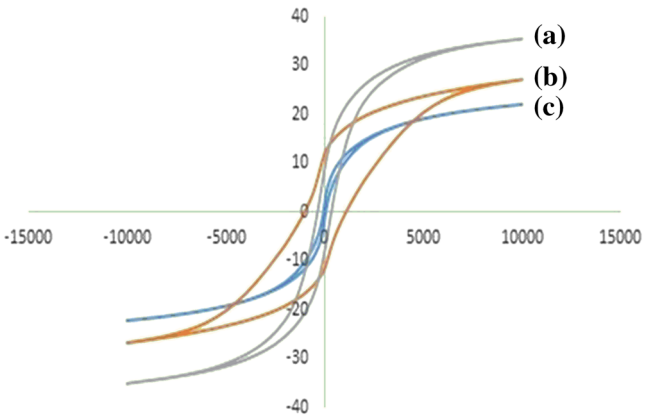


**FIGURE 6** Vibrating sample magnetometry curves: (a) $CoFe_2O_4@SiO_2$, (b) $CoFe_2O_4@SiO_2@Si-(CH_2)_3Cl$, and (c) $CoFe_2O_4@SiO_2@Si-(CH_2)_3Cl@NA$ nanocatalyst

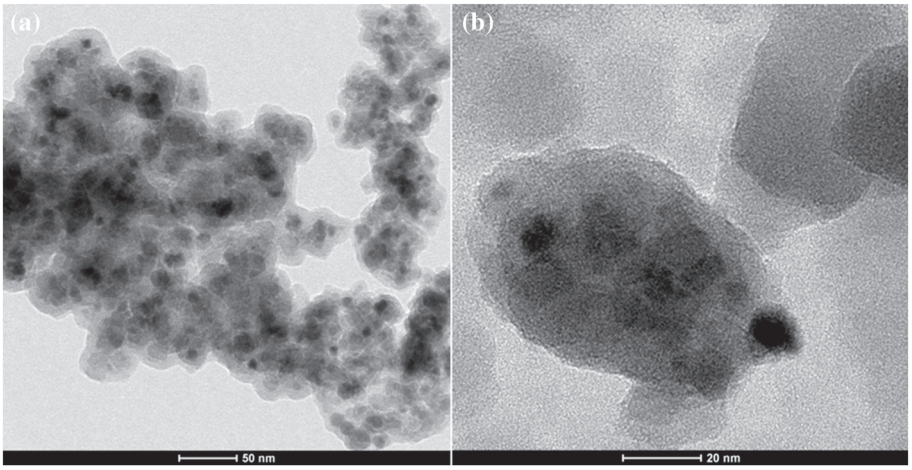


**FIGURE 5** High-resolution transmission electron microscopy images of the prepared $CoFe_2O_4@SiO_2@Si-(CH_2)_3Cl@NA$ magnetic nanoparticles

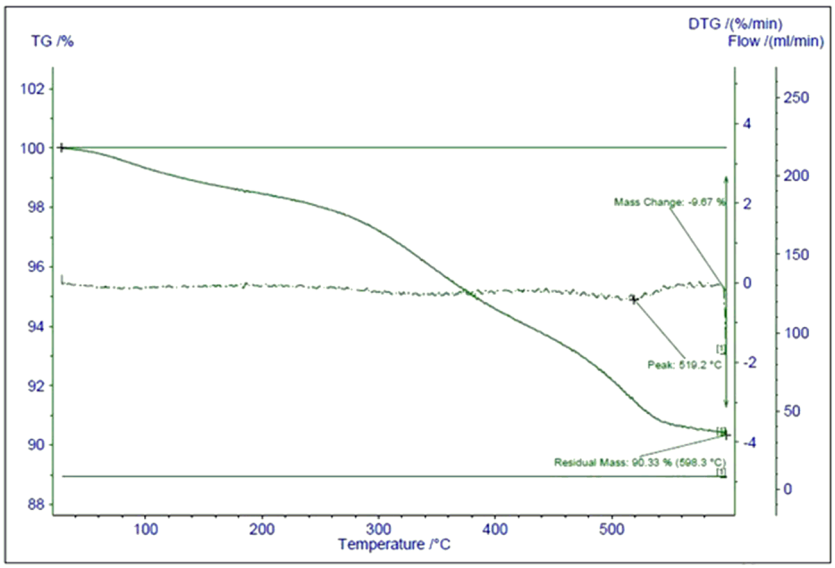


**FIGURE 7** Thermogravimetric analysis thermogram of the $CoFe_2O_4$@$SiO_2$@Si-$(CH_2)_3$Cl@NA nanocatalyst. DTG, differential thermogravimetry

nanocomposite was successfully prepared according to procedure presented in Scheme 2.

The FT-IR spectra of the $CoFe_2O_4$, $CoFe_2O_4$@$SiO_2$, $CoFe_2O_4$@$SiO_2$@Si-$(CH_2)_3$Cl, and $CoFe_2O_4$@$SiO_2$@Si-$(CH_2)_3$@NA are shown in Figure 1. The wavenumber 587 $cm^{-1}$ corresponds to the stretching vibration of Co–O, and bands at 1635 and 3408 $cm^{-1}$ correspond to the OH stretching vibration of hydroxides, which confirms the formation of $CoFe_2O_4$ (Figure 1a).[36]. The band at 1087 $cm^{-1}$ is related to the Si–O group of $SiO_2$ in $CoFe_2O_4$@$SiO_2$ (Figure 1b), the band at 2931 $cm^{-1}$ represents the $CH_2$ stretching of propyl chloride in $CoFe_2O_4$@$SiO_2$@Si-$(CH_2)_3$Cl (Figure 1c), and bands at 1728 and 3416 $cm^{-1}$ correspond to the C=O and OH stretching of nicotinic acid in $CoFe_2O_4$@$SiO_2$@Si-$(CH_2)_3$Cl@NA, respectively (Figure 1d).

## 3.2 | X-ray diffraction analysis

The X-ray diffraction (XRD) patterns of $CoFe_2O_4$@$SiO_2$, $CoFe_2O_4$@$SiO_2$@Si-$(CH_2)_3$Cl, and $CoFe_2O_4$@$SiO_2$@Si-$(CH_2)_3$Cl@NA are presented in Figure 2. The XRD patterns of $CoFe_2O_4$@$SiO_2$, $CoFe_2O_4$@$SiO_2$@Si-$(CH_2)_3$Cl, and $CoFe_2O_4$@$SiO_2$@Si-$(CH_2)_3$@NA illustrated main peaks at $2\theta$ = 30.12°, 35.45°, 43.3°, 53.89°, 57.20°, and 62.72°. The XRD patterns for $CoFe_2O_4$@$SiO_2$@Si-$(CH_2)_3$@NA revealed peaks indicative of pure $CoFe_2O_4$ nanoparticles with a spinel structure.[37] According to the Debye–Scherrer equation for the full width at half maximum of the sharpest diffraction peak (311), the average crystallite size for $CoFe_2O_4$@$SiO_2$, $CoFe_2O_4$@$SiO_2$@Si-$(CH_2)_3$Cl, and $Fe_3O_4$@$SiO_2$@Si-$(CH_2)_3$Cl@NA was 13, 18, and 19 nm, respectively.

## 3.3 | SEM analysis

Surface morphological image of the $Fe_3O_4$@$SiO_2$@Si-$(CH_2)_3$Cl@NA nanocatalyst explored by a scanning electron microscope is presented in Figure 3. The average size of the fine nonagglomerated particles was found to be nearly 23 nm. This confirms the nanostructure of the nanocatalyst.

In addition, the EDS spectrum of the $Fe_3O_4$@$SiO_2$@Si-$(CH_2)_3$Cl@NA nanocomposite shows the presence of carbon (C), nitrogen (N), oxygen (O), silicon (Si), iron (Fe), and cobalt (Co) components in the nanocomposite (Figure 4).

## 3.4 | HRTEM analysis

The structural information about the nicotinic acid-supported cobalt ferrite [$CoFe_2O_4$/$SiO_2$@Si$(CH_2)_3$Cl@NA] was investigated by HRTEM. HRTEM

**TABLE 1** Synthesis of **4a** using different solvents[a]

| Entry | Solvent | Time (hr) | Yield (%)[b] |
|---|---|---|---|
| 1 | Ethanol | 3 | 70 |
| 2 | Ethyl acetate | 7 | 40 |
| 3 | *n*-Hexane | 8 | 35 |
| 4 | $CHCl_3$ | 3 | 95 |
| 5 | MeCN | 4 | 65 |

[a]Reaction conditions: 4-Cl-benzaldehyde (1 mmol), 4-aminocoumarin (1 mmol), 1,3-cyclohexadione (1 mmol), and $CoFe_2O_4$@$SiO_2$@Si-$(CH_2)_3$Cl@NA (0.02 g) under reflux conditions.
[b]Yield refers to isolated products.

**TABLE 2** Synthesis of chromeno[3,4-*b*]quinolines catalyzed by the $Fe_3O_4$@$SiO_2$@Si-$(CH_2)_3$Cl@NA nanocatalyst[a]

| Entry | Ar | R | Product | Time (hr) | Yield (%)[b] | Melting point (°C) |
|---|---|---|---|---|---|---|
| 1 | 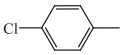 | H | **4a** | 3 | 95 | 216–218 |
| 2 | 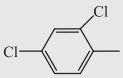 | H | **4b** | 2.45 | 96 | 284–286 |
| 3 | 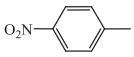 | H | **4c** | 2.5 | 97 | 262–264 |
| 4 | 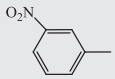 | H | **4d** | 3 | 96 | 298–300 |
| 5 | 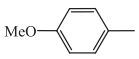 | H | **4e** | 4 | 91 | 278–280 |
| 6 | 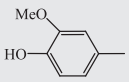 | H | **4f** | 4 | 90 | 336–338 |
| 7 | 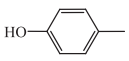 | H | **4g** | 4 | 92 | 335–337 |
| 8 | 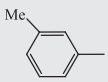 | H | **4h** | 4.5 | 90 | 304–306 |
| 9 | 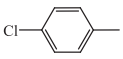 | Me | **4i** | 3 | 94 | 301–303 |
| 10 | 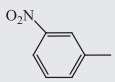 | Me | **4j** | 3.5 | 94 | 282–284 |
| 11 | 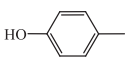 | Me | **4k** | 4 | 92 | 348–350 |
| 12 | 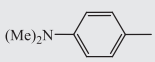 | Me | **4l** | 5 | 90 | 160–161 |
| 13 |  | Me | **4m** | 4 | 91 | 300–302 |
| 14 | | Me | **4n** | 3 | 90 | 264–266 |

(Continues)

**TABLE 2** (Continued)

| Entry | Ar | R | Product | Time (hr) | Yield (%)[b] | Melting point (°C) |
|---|---|---|---|---|---|---|
| | 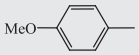 | | | | | |
| 15 | 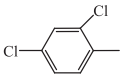 | Me | **4o** | 3 | 96 | 333–334 |
| 16 | 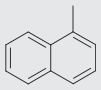 | Me | **4p** | 5 | 93 | 322–324 |

[a]Reaction conditions: Aldehyde (1 mmol), 4-aminocoumarin (1 mmol), dimedone or 1,3-cyclohexadione (1 mmol), and $CoFe_2O_4@SiO_2@Si\text{-}(CH_2)_3Cl@NA$ (0.02 g) in $CHCl_3$ under reflux conditions.
[b]Yield refers to isolated products.

images of the synthesized nicotinic acid-supported cobalt ferrite show the formation of the $CoFe_2O_4@SiO_2@Si(CH_2)_3Cl@NA$ core–shell nanostructure. The HRTEM image of $CoFe_2O_4/SiO_2@Si(CH_2)_3Cl@NA$ shows highly uniform crystalline spherical nanoparticles with grain size of about 20–30 nm (Figure 5a).

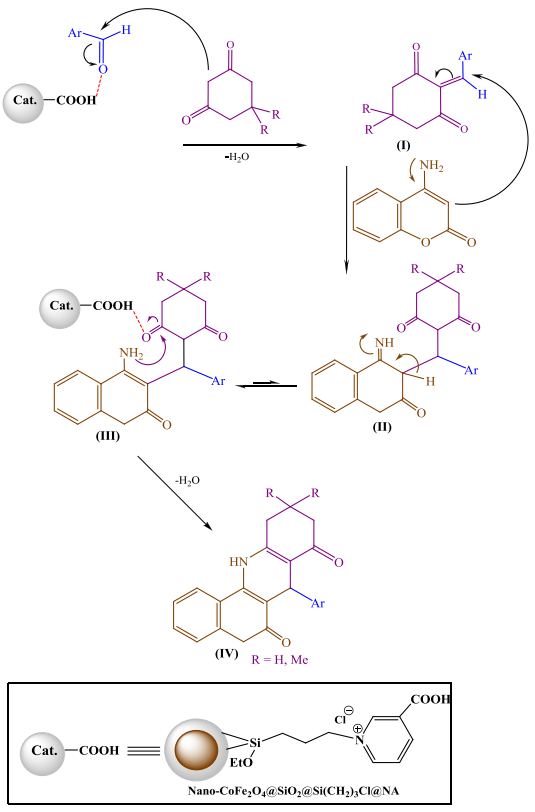


**SCHEME 3** Plausible mechanism for the synthesis of chromeno[3,4-*b*]quinoline derivatives by $CoFe_2O_4@SiO_2@Si\text{-}(CH_2)_3Cl@NA$

## 3.5 | Vibrating sample magnetometry analysis

Magnetic properties of $CoFe_2O_4$, $CoFe_2O_4@SiO_2$, $CoFe_2O_4@SiO_2@Si\text{-}(CH_2)_3Cl$, and $Fe_3O_4@SiO_2@Si\text{-}(CH_2)_3Cl@NA$ nanocatalyst were characterized by vibrating sample magnetometry. In general, magnetization increased with increases in the magnetic field. The magnetic hysteresis loops of $CoFe_2O_4@SiO_2$, $CoFe_2O_4@SiO_2@Si\text{-}(CH_2)_3Cl$, and $CoFe_2O_4@SiO_2@Si\text{-}(CH_2)_3Cl@NA$ are provided in Figure 6a–c. The saturation magnetization value of the pristine $CoFe_2O_4@SiO_2$ nanoparticles was 35.47 emu/g. This high saturation magnetization value indicates a good crystal structure. The saturation magnetization values of $CoFe_2O_4@SiO_2@Si\text{-}(CH_2)_3Cl$ and $Fe_3O_4@SiO_2@Si\text{-}(CH_2)_3Cl@NA$ were 27.17 and 22.07 emu/g, respectively (Figure 6c). Although the saturation magnetization of the catalyst was lower than that of $CoFe_2O_4@SiO_2@Si\text{-}(CH_2)_3Cl$ (Figure 6b), this was sufficient enough to recover the catalyst easily from the reaction mixture.

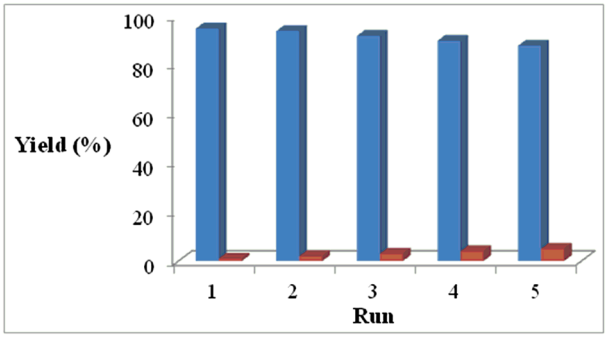


**FIGURE 8** Recyclability of the catalyst for the synthesis of **4a**

**TABLE 3** Comparison of $Fe_3O_4$@$SiO_2$@Si-$(CH_2)_3$Cl@NA with some other catalysts for the synthesis of **4c** and **4n**

| Entryproduct | Catalyst | Reaction conditions | Time/min | Yield (%) | Reference |
|---|---|---|---|---|---|
| **4c** | – | 200–220 °C | 45 | 45 | [38] |
| **4c** | Cu(II)–Schiff base/SBA-15 | 200 °C | 5 | 70 | [33] |
| **4c** | $Fe_3O_4$@$SiO_2$@Si-$(CH_2)_3$Cl@NA | $CHCl_3$/reflux | 150 | 97 | This work |
| **4n** | – | *n*-PrOH/reflux | 720 | 72 | [39] |
| **4n** | (±)Lactic acid | Ethyl-L-lactate/100 °C | 180 | 78 | [32] |
| **4n** | $Fe_3O_4$@$SiO_2$@Si-$(CH_2)_3$Cl@NA | $CHCl_3$/reflux | 180 | 90 | This work |

## 3.6 | Thermogravimetric analysis

The thermal behavior of the $Fe_3O_4$@$SiO_2$@Si-$(CH_2)_3$Cl@NA nanocatalyst is presented in Figure 6. According to the TGA thermogram of the nanocatalyst, a weight loss of about 9.67% occurred at 598 °C (Figure 7). Thus, the catalyst remains stable and decomposes only above 600 °C.

To optimize the reaction conditions, the reaction between 4-chlorobenzaldehyde, 4-aminocoumarin, and 1,3-cyclohexadione was examined as a model reaction in several solvents, including ethanol, *n*-hexane, ethyl acetate, chloroform, and acetonitrile (Table 1). Among these, chloroform under reflux conditions was more efficient with respect to reaction time and yield of the desired product (Table 1).

To investigate the effect of catalyst loading, the model reaction was carried out in the presence of different amounts of catalyst (0.01, 0.02, and 0.03 g). It was observed that the variation of amount of $CoFe_2O_4$@$SiO_2$@Si-$(CH_2)_3$@NA had an effective influence, with 0.02 g identified to be the best amount of $CoFe_2O_4$@$SiO_2$@Si-$(CH_2)_3$Cl@NA, as this afforded the desired product in 95% yields. After optimization of the reaction conditions, a variety of chromeno[3,4-*b*]quinoline derivatives were synthesized by $Fe_3O_4$@$SiO_2$@Si-$(CH_2)_3$Cl@NA in $CHCl_3$ under reflux conditions (Table 2, Entries 1–16). The reactions worked well with all arylaldehydes with electron-donating or electron-withdrawing substituent.

Mechanistic pathway indicates the catalytic role of $Fe_3O_4$@$SiO_2$@Si-$(CH_2)_3$Cl@NA in the synthesis of chromeno[3,4-*b*]quinoline derivatives (Scheme 3). Electrophilicity of the carbonyl group of aldehyde is increased by hydrogen bonding with acidic hydrogen of the catalyst. It is supposed that the reaction may proceed at first by the reaction of aldehyde with dimedone or 1,3-cyclohexadione, which provides the desired Knoevenagel intermediate **I**. Then, 4-aminocoumarin attacks intermediate **I** to produce intermediate **II**. Afterward, intermediate **II** is converted into intermediate **III** by tautomerization. Finally, intermediate **III** generates product **IV** by dehydration.

The magnetic property of $Fe_3O_4$@$SiO_2$@Si-$(CH_2)_3$Cl@NA facilitates its efficient recovery from the reaction mixture during work-up. The activity of the recycled catalyst was also examined under the reaction conditions. After the completion of reaction, the catalyst was separated by an external magnet, washed with ethanol, and dried. The recovered catalyst was reused for five consecutive cycles without significant loss in its catalytic activity (Figure 8). However, beyond five runs the activity of the catalyst was reduced, and thus required re-functionalization with nicotinic acid.

To study the efficiency of the present method for the synthesis of chromeno[3,4-*b*]quinoline derivatives, compounds **4c** and **4n** were compared with some of those reported in the literature (Table 3). As can be seen, when all conditions including efficiency and reaction conditions are considered, our results present a good comparison with previously reported data.

## 4 | CONCLUSIONS

In this research, for the first time, $Fe_3O_4$@$SiO_2$@Si-$(CH_2)_3$Cl@NA as a recyclable magnetic nanocatalyst was prepared. In the prepared $Fe_3O_4$@$SiO_2$@Si-$(CH_2)_3$Cl@NA nanostructure, the cobalt ferrite component was responsible for the magnetic recyclable ability. The silica shell as the intermediate layer aids in stabilizing and protecting the cobalt ferrite part. The outermost nicotinic acid component acts as the catalyst for the one-pot synthesis of chromeno[3,4-*b*]quinoline derivatives by the reaction of aldehydes, dimedone or 1,3-cyclohexadione, and 4-aminocoumarin. FT-IR, EDS, and XRD results as well as FESEM and HRTEM images indicated that the $Fe_3O_4$@$SiO_2$@Si-$(CH_2)_3$Cl@NA nanocatalyst can be successfully prepared via the utilized route. Furthermore, the $Fe_3O_4$@$SiO_2$@Si-$(CH_2)_3$Cl@NA nanocatalyst showed excellent recycling efficiency as well as stability for at least five runs. The high efficiency, one-pot synthesis, excellent yields over appropriate reaction times, and affordable procedure are some of the advantages of this method.

Spectroscopic data for synthetic compounds are given in the following sections.

### 4.1 | 7-(4-Chlorophenyl)-7,10,11,12-tetrahydro-6*H*-chromeno[4,3-*b*]quinoline-6,8(9*H*)-dione (4a)

MP: 216–218 °C; FT-IR (KBr, $\nu$, $cm^{-1}$): 3435, 2958, 2929, 2866, 1727, 1632, 1473, 1361, 1280, 1174, 1129, 1073, 1035, 919, 830, 756. $^1$H NMR (300 MHz, DMSO-$d_6$): δ 9.80 (s, 1H, NH), 8.33 (d, $J$ = 7.8 Hz, 1H, Ar–H), 7.64 (t, $J$ = 7.5 Hz, 1H, Ar–H), 7.39–7.49 (m, 2H, Ar–H), 7.27–7.37 (m, 4H, Ar–H), 5.00 (s, 1H, CH), 2.71–2.91 (m, 2H, $CH_2$), 2.30–2.34 (m, 2H, $CH_2$), 1.85–2.06 (m, 2H, $CH_2$). $^{13}$C NMR (75 MHz, DMSO-$d_6$): δ 195.4, 160.8, 152.4, 151.5, 149.5, 141.9, 134.7, 132.1, 128.6, 124.3, 123.2, 117.2, 113.6, 112.8, 112.7, 102.9, 37.2, 33.3, 26.8, 21.3. Anal. calcd for $C_{22}H_{16}NO_3Cl$: C 69.94, H 4.27, N 3.71. Found: C 70.03, H 4.30, N 3.77.

### 4.2 | 7-(2,4-Dichlorophenyl)-7,10,11,12-tetrahydro-6*H*-chromeno[4,3-*b*]quinoline-6,8(9*H*)-dione (4b)

MP: 284–286 °C; FT-IR (KBr, $\nu$, $cm^{-1}$): 3285, 3085, 2952, 1704, 1633, 1605, 1505, 1475, 1359, 1245, 1180, 1140, 1073, 1036, 921, 846, 755. $^1$H NMR (300 MHz, DMSO-$d_6$): δ 9.78 (s, 1H, NH), 8.33 (d, $J$ = 7.8 Hz, 1H, Ar–H), 7.64 (t, $J$ = 7.8 Hz, 1H, Ar–H), 7.37–7.49 (m, 4H, Ar–H), 7.27 (d, $J$ = 8.1 Hz, 1H, Ar–H), 5.27 (s, 1H, CH), 2.66–2.91 (m, 2H, $CH_2$), 2.18–2.34 (m, 2H, $CH_2$), 1.78–1.99 (m, 2H, $CH_2$). $^{13}$C NMR (75 MHz, DMSO-$d_6$): δ 195.4, 160.3, 152.6, 143.0, 142.7, 134.1, 133.9, 132.6, 131.7, 128.8, 127.3, 124.4, 123.5, 117.3, 113.1, 111.5, 101.1, 37.1, 34.4, 26.8, 21.1. Anal. calcd for $C_{22}H_{15}NO_3Cl_2$: C 64.09, H 3.67, N 3.40. Found: C 64.11, H 3.70, N 3.38.

### 4.3 | 7-(4-Nitrophenyl)-7,10,11,12-tetrahydro-6*H*-chromeno[4,3-*b*]quinoline-6,8(9*H*)-dione (4c)

MP: 262–264 °C; FT-IR (KBr, $\nu$, $cm^{-1}$): 3314, 3093, 2949, 2868, 1677, 1634, 1604, 1513, 1469, 1347, 1243, 1167, 1202, 1136, 1110, 1049, 920, 896, 856, 822, 756. $^1$H NMR (300 MHz, DMSO-$d_6$): δ 9.89 (s, 1H, NH), 8.36 (d, $J$ = 7.5 Hz, 1H, Ar–H), 8.10 (d, $J$ = 7.8 Hz, 2H, Ar–H), 7.66 (t, $J$ = 7.2 Hz, 1H, Ar–H), 7.40–7.56 (m, 4H, Ar–H), 5.12 (s, 1H, CH), 2.72–2.92 (m, 2H, $CH_2$), 2.30–2.34 (m, 2H, $CH_2$), 1.90–2.01 (m, 2H, $CH_2$). $^{13}$C NMR (75 MHz, DMSO-$d_6$): δ 195.4, 160.7, 153.6, 152.7, 152.6, 146.4, 143.0, 132.6, 129.6, 124.5, 123.7, 123.5, 117.3, 113.3, 111.4, 101.1, 37.0, 35.5, 26.8, 21.1. Anal. calcd for $C_{22}H_{16}N_2O_5$: C 68.04, H 4.15, N 7.21; found: C 68.07, H 4.17, N 7.24.

### 4.4 | 7-(3-Nitrophenyl)-7,10,11,12-tetrahydro-6*H*-chromeno[4,3-*b*]quinoline-6,8(9*H*)-dione (4d)

MP: 298–300 °C; FT-IR (KBr, $\nu$, $cm^{-1}$): 3289, 3097, 2927, 1677, 1713, 1631, 1605, 1528, 1507, 1475, 1352, 1167, 1246, 1186, 1142, 1075, 1031, 927, 760. $^1$H NMR (300 MHz, DMSO-$d_6$): δ 9.91 (s, 1H, NH), 8.35 (d, $J$ = 7.5 Hz, 1H, Ar–H), 8.10 (d, $J$ = 7.8 Hz, 2H, Ar–H), 8.08 (s, 1H), 8.00 (d, $J$ = 7.5 Hz, 1H, Ar–H), 7.65–7.74 (m, 2H, Ar–H), 7.39–7.57 (m, 3H, Ar–H), 5.12 (s, 1H, CH), 2.75–2.91 (m, 2H, $CH_2$), 2.26–2.36 (m, 2H, $CH_2$), 1.90–2.06 (m, 2H, $CH_2$). $^{13}$C NMR (75 MHz, DMSO-$d_6$): δ 195.5, 160.7, 152.8, 152.6, 148.3, 148.0, 143.0, 132.6, 130.0, 124.5, 123.5, 122.7, 117.3, 113.2, 111.5, 101.3, 36.9, 35.3, 26.8, 21.1. Anal. calcd for $C_{22}H_{16}N_2O_5$: $C_{22}H_{16}N_2O_5$: C 68.04, H 4.15, N 7.21; found: C 68.09, H 4.20, N 7.25.

### 4.5 | 7-(4-Methoxyphenyl)-7,10,11,12-tetrahydro-6*H*-chromeno[4,3-*b*]quinoline-6,8(9*H*)-dione (4e)

MP: 278–280 °C; FT-IR (KBr, $\nu$, $cm^{-1}$): 3322, 3077, 2935, 2837, 1677, 1640, 1508, 1470, 1363, 1304, 1241, 1179, 1138, 1032, 920, 753. $^1$H NMR (300 MHz, DMSO-$d_6$): δ 9.75 (s, 1H, NH), 8.32 (d, $J$ = 7.5 Hz, 1H, Ar–H), 7.64 (t, $J$ = 7.2 Hz, 1H, Ar–H), 7.39–7.49 (m, 2H, Ar–H), 7.12 (d, $J$ = 7.8 Hz, 2H, Ar–H), 7.01 (d, $J$ = 7.8 Hz, 2H, Ar–H), 4.98 (s, 1H, CH), 3.68 (s, 3H, OMe), 2.73–2.89 (m, 2H, $CH_2$), 2.30 (sbr, 2H, $CH_2$), 1.89–2.01 (m, 2H, $CH_2$). $^{13}$C NMR (75 MHz, DMSO-$d_6$): δ 195.4, 160.8, 158.1, 152.4, 151.8, 142.2, 138.7, 132.3, 129.1, 124.4, 123.3, 117.3, 113.8, 113.5, 112.6, 102.5, 56.1, 37.1, 33.7, 26.8, 21.2. Anal. calcd for $C_{23}H_{19}NO_4$: C 73.98, H 5.13, N 3.75; found: 74.06, H 5.16, N 3.76.

### 4.6 | 7-(4-Hydroxy-3-methoxyphenyl)-7,10,11,12-tetrahydro-6*H*-chromeno[4,3-*b*]quinoline-6,8 (9*H*)-dione (4f)

MP: 336–338 °C; (KBr, $\nu$, $cm^{-1}$): 3362, 3059, 2945, 1696, 1625, 1509, 1469, 1360, 1274, 1237, 1178, 1032, 902, 765. $^1$H NMR (300 MHz, DMSO-$d_6$): δ 9.72 (s, 1H, NH), 8.29 (d, $J$ = 7.5 Hz, 1H, Ar–H), 7.60 (t, $J$ = 7.2 Hz, 1H, Ar–H), 7.37–7.46 (m, 2H, Ar–H); 6.88 (d, $J$ = 1.5 Hz, 1H, Ar–H),

6.55–6.64 (m, 2H, Ar–H), 4.94 (s, 1H, CH), 2.66–2.90 (m, 2H, $CH_2$), 2.31–2.34 (m, 2H, $CH_2$), 1.91–2.08 (m, 2H, $CH_2$). $^{13}$C NMR (75 MHz, DMSO-$d_6$): δ 195.5, 160.0, 152.4, 151.8, 147.4, 145.5, 137.5, 132.2, 124.4, 123.3, 120.0, 117.2, 115.6, 113.6, 112.8, 112.4, 102.6, 56.0, 37.2, 33.7, 26.8, 21.3. Anal. calcd for $C_{23}H_{19}NO_5$: C 70.94, H 4.92, N 3.60; found: 70.96, H 4.90, N 3.62.

### 4.7 | 7-(4-Hydroxyphenyl)-7,10,11,12-tetrahydro-6*H*-chromeno[4,3-*b*]quinoline-6,8(9*H*)-dione (4g)

MP: 335–337 °C; (KBr, $\nu$, cm$^{-1}$): 3343, 2926, 1672, 1634, 1607, 1511, 1473, 1366, 1264, 1243, 1174, 1036, 923, 755. $^1$H NMR (300 MHz, DMSO-$d_6$): δ 9.68 (s, 1H, NH), 9.17 (s, 1H, OH), 8.29 (d, $J$ = 7.8 Hz, 1H, Ar–H), 7.58 (t, $J$ = 7.5 Hz, 1H, Ar–H), 7.34–7.44 (m, 2H, Ar–H), 7.03 (d, $J$ = 8.1 Hz, 2H, Ar–H), 6.60 (d, $J$ = 8.1 Hz, 2H, Ar–H), 4.91 (s, 1H, CH), 2.65–2.89 (m, 2H, $CH_2$), 2.30 (sbr, 2H, $CH_2$), 1.86–2.06 (m, 2H, $CH_2$). $^{13}$C NMR (75 MHz, DMSO-$d_6$): δ 195.4, 160.8, 156.2, 152.4, 151.7, 142.0, 137.1, 132.1, 129.0, 124.3, 123.3, 117.2, 115.2, 113.5, 112.7, 102.7, 37.2, 33.5, 26.8, 21.2. Anal. calcd for $C_{22}H_{17}NO_4$: C 73.53, H 4.77, N 3.90; found: 73.56, H 4.80, N 3.93.

### 4.8 | 7-(*m*-Tolyl)-7,10,11,12-tetrahydro-6*H*-chromeno[4,3-*b*]quinoline-6,8(9*H*)-dione (4h)

MP: 304–306 °C; (KBr, $\nu$, cm$^{-1}$): 3309, 3042, 2947, 1685, 1634, 1606, 1572, 1506, 1475, 1362, 1241, 1189, 1169, 1142, 1040, 925, 754. $^1$H NMR (300 MHz, DMSO-$d_6$): δ 9.76 (s, 1H, NH), 8.32 (d, $J$ = 7.5 Hz, 1H, Ar–H), 7.63 (t, $J$ = 7.2 Hz, 1H, Ar–H), 7.39–7.48 (m, 2H, Ar–H), 6.92–7.13 (m, 4H, Ar–H), 4.98 (s, 1H, CH), 2.71–2.91 (m, 2H, $CH_2$), 2.52 (s, 3H, $CH_3$), 2.23–2.32 (m, 2H, $CH_2$), 1.90–2.02 (m, 2H, $CH_2$). $^{13}$C NMR (75 MHz, DMSO-$d_6$): δ 195.4, 160.8, 152.5, 152.0, 146.3, 142.4, 137.3, 132.3, 128.7, 128.4, 127.3, 125.2, 123.4, 117.3, 113.5, 112.4, 102.3, 37.1, 34.5, 26.8, 21.6, 21.2. Anal. calcd for $C_{23}H_{19}NO_3$: C 77.29, H 5.36, N 3.92; found: 77.33, H 5.38, N 3.90.

### 4.9 | 7-(4-Chlorophenyl)-10,10-dimethyl-7,10,11,12-tetrahydro-6*H*-chromeno[4,3-*b*]quinoline-6,8(9*H*)-dione (4i)

MP: 301–303 °C; (KBr, $\nu$, cm$^{-1}$): 3294, 3076, 2945, 1704, 1633, 1608, 1571, 1506, 1475, 1361, 1303, 1238, 1193, 1149, 1020, 919, 892, 842, 754. $^1$H NMR (300 MHz, DMSO-$d_6$): δ 9.96 (s, 1H, NH), 8.42 (d, $J$ = 6.6 Hz, 1H, Ar–H), 7.57 (t, $J$ = 7.2 Hz, 1H, Ar–H), 7.32–7.43 (m, 2H, Ar–H), 7.26 (sbr, 4H, Ar–H), 4.94 (s, 1H, CH), 2.61–2.77 (m, 2H, $CH_2$), 2.24 (d, $J$ = 16.2 Hz, 1H, $CH_2$), 2.05 (d, $J$ = 16.2 Hz, 1H, $CH_2$), 1.06 (s, 3H, $CH_3$), 0.92 (s, 3H, $CH_3$). $^{13}$C NMR (75 MHz, DMSO-$d_6$): δ 195.1, 160.7, 152.5, 150.6, 145.2, 142.9, 132.4, 131.2, 130.1, 128.3, 124.4, 123.9, 117.2, 113.5, 110.8, 101.7, 50.5, 34.6, 32.6, 29.5, 26.9. Anal. calcd for $C_{24}H_{20}NO_3Cl$: C 71.02, H 4.97, N 3.45; found: 71.06, H 4.93, N 3.48.

### 4.10 | 10,10-Dimethyl-7-(3-nitrophenyl)-7,10,11,12-tetrahydro-6*H*-chromeno[4,3-*b*]quinoline-6,8 (9*H*)-dione (4j)

MP: 282–284 °C; (KBr, $\nu$, cm$^{-1}$): 3221, 3089, 2930, 1727, 1651, 1604, 1509, 1471, 1366, 1345, 1290, 1235, 1192, 1149, 1044, 894, 760. $^1$H NMR (300 MHz, DMSO-$d_6$): δ 9.85 (s, 1H, NH), 8.33 (d, $J$ = 6.6 Hz, 1H, Ar–H), 8.00 (m, 2H, Ar–H), 7.37–7.72 (m, 4H, Ar–H), 5.07 (s, 1H, CH), 2.52–2.71 (m, 2H, $CH_2$), 2.28 (d, $J$ = 15.6 Hz, 1H, $CH_2$), 2.08 (d, $J$ = 15.6 Hz, 1H, $CH_2$), 1.09 (s, 3H, $CH_3$), 0.95 (s, 3H, $CH_3$). $^{13}$C NMR (75 MHz, DMSO-$d_6$): δ 195.1, 160.7, 152.6, 150.8, 148.1, 148.0, 143.0, 135.1, 132.7, 130.0, 124.6, 123.6, 122.7, 121.8, 117.4, 113.3, 110.5, 101.4, 50.3, 35.5, 32.6, 29.5, 26.9. Anal. calcd for $C_{24}H_{20}N_2O_5$: C 69.22, H 4.84, N 6.73; found: 69.26, H 4.81, N 6.68.

### 4.11 | 7-(4-Hydroxyphenyl)-10,10-dimethyl-7,10,11,12-tetrahydro-6*H*-chromeno[4,3-*b*]quinoline-6,8(9*H*)-dione (4k)

MP: 348–350 °C; (KBr, $\nu$, cm$^{-1}$): 3280, 3242, 3054, 2951, 1719, 1632, 1588, 1508, 1476, 1362, 1305, 1243, 1193, 1145, 1039, 1014, 920, 838, 756. $^1$H NMR (300 MHz, DMSO-$d_6$): δ 9.62 (s, 1H, NH), 9.17 (s, 1H, OH), 8.27 (d, $J$ = 7.2 Hz, 1H, Ar–H), 7.57 (t, $J$ = 8.4 Hz, 1H, Ar–H), 7.33–7.44 (m, 2H, Ar–H), 7.03 (d, $J$ = 8.4 Hz, 2H, Ar–H), 6.59 (d, $J$ = 8.4 Hz, 2H, Ar–H), 4.86 (s, 1H, CH), 2.65 (sbr, 2H, $CH_2$), 2.25 (d, $J$ = 16.2 Hz, 1H, $CH_2$), 2.06 (d, $J$ = 16.2 Hz, 1H, $CH_2$), 1.08 (s, 3H, $CH_3$), 0.96 (s, 3H, $CH_3$). $^{13}$C NMR (75 MHz, DMSO-$d_6$): δ 195.1, 160.7, 156.2, 152.4, 149.6, 142.1, 137.0, 132.1, 129.1, 124.4, 123.3, 117.2, 115.1, 113.5, 111.6, 102.7, 50.6, 33.8, 32.6, 29.6, 26.9. Anal. calcd for $C_{24}H_{21}NO_4$: C 74.40, H 5.46, N 3.62; found: 74.46, H 5.43, N 3.60.

### 4.12 | 7-[4-(Dimethylamino)phenyl]-10,10-dimethyl-7,10,11,12-tetrahydro-6*H*-chromeno[4,3-*b*] quinoline-6,8(9*H*)-dione (4l)

MP: 160–161 °C; (KBr, $\nu$, $cm^{-1}$): 3297, 3073, 2957, 1696, 1661, 1511, 1477, 1345, 1312, 1242, 1196, 1150, 1106, 1053, 829, 753. $^1$H NMR (300 MHz, DMSO-$d_6$): δ 9.83 (s, 1H, NH), 8.33 (d, $J$ = 7.8 Hz, 1H, Ar–H), 8.10 (d, $J$ = 8.4 Hz, 2H, Ar–H), 7.64 (t, 1H, $J$ = 7.5 Hz, Ar–H), 7.50 (d, $J$ = 8.4 Hz, 2H, Ar–H), 7.38–7.47 (m, 2H, Ar–H), 5.07 (s, 1H, CH), 2.90 (s, 3H, $NCH_3$), 2.74 (s, 3H, $NCH_3$), 2.52–2.69 (m, 2H, $CH_2$), 2.27 (d, $J$ = 16.2 Hz, 1H, $CH_2$), 2.07 (d, $J$ = 16.2 Hz, 1H, $CH_2$), 1.08 (s, 3H, $CH_3$), 0.94 (s, 3H, $CH_3$). $^{13}$C NMR (75 MHz, DMSO-$d_6$): δ 195.1, 162.7, 160.6, 153.5, 152.6, 150.8, 146.4, 143.2, 132.7, 129.6, 124.6, 123.7, 123.6, 117.4, 113.3, 110.3, 101.1, 50.4, 36.2, 35.7, 32.6, 31.2, 29.4, 27.0. Anal. calcd for $C_{26}H_{26}N_2O_3$: C 75.34, H 6.32, N 6.76; found: 75.36, H 6.28, N 6.78.

### 4.13 | 7-(2-Chlorophenyl)-10,10-dimethyl-7,10,11,12-tetrahydro-6*H*-chromeno[4,3-*b*] quinoline-6,8 (9*H*)-dione (4m)

MP: 300–302 °C; (KBr, $\nu$, $cm^{-1}$): 3292, 3075, 2956, 1711, 1633, 1607, 1510, 1475, 1364, 1243, 1198, 1148, 1041, 1021, 757. $^1$H NMR (300 MHz, DMSO-$d_6$): δ 9.72 (s, 1H, NH), 8.34 (d, $J$ = 6.9 Hz, 1H, Ar–H), 7.63 (t, $J$ = 8.4 Hz, 1H, Ar–H), 7.40 (t, $J$ = 8.1 Hz, 1H, Ar–H), 7.36–7.39 (m, 2H, Ar–H),7.25 (dd, 1H, $J$ = 7.5, 1.5 Hz, Ar–H), 7.17 (td, $J$ = 7.2, 1.8 Hz, 1H, Ar–H), 7.10–7.15 (m, 1H, Ar–H), 5.28 (s, 1H, CH), 2.53 (sbr, 2H, $CH_2$), 2.23 (d, $J$ = 16.2 Hz, 1H, $CH_2$), 2.00 (d, $J$ = 16.2 Hz, 1H, $CH_2$), 1.08 (s, 3H, $CH_3$), 0.95 (s, 3H, $CH_3$). $^{13}$C NMR (75 MHz, DMSO-$d_6$): δ 194.8, 160.3, 152.6, 150.4, 143.3, 143.0, 133.1, 132.7, 132.5, 129.7, 128.2, 127.0, 124.4, 117.2, 113.2, 110.6, 101.4, 50.6, 34.7, 32.4, 29.5, 26.9. Anal. calcd for $C_{24}H_{20}NO_3Cl$: C 71.02, H 4.97 N 3.45; found: 70.96, H 4.93, N 3.48.

### 4.14 | 7-(4-Methoxyphenyl)-10,10-dimethyl-7,10,11,12-tetrahydro-6*H*-chromeno[4,3-*b*]quinoline-6,8(9*H*)-dione (4n)

MP: 264–266 °C; (KBr, $\nu$, $cm^{-1}$): 3263, 3093, 2958, 1727, 1646, 1606, 1511, 1471, 1365, 1261, 1237, 1196, 1039, 1021, 752. $^1$H NMR (300 MHz, DMSO-$d_6$): δ 9.68 (s, 1H, NH), 8.32 (d, $J$ = 7.5 Hz, 1H, Ar–H), 7.64 (t, $J$ = 7.2 Hz, 1H, Ar–H), 7.39–7.49 (m, 2H, Ar–H), 7.15 (d, $J$ = 7.8 Hz, 2H, Ar–H), 6.7 (d, $J$ = 7.8 Hz, 2H, Ar–H), 4.90 (s, 1H, CH), 3.67 (s, 3H, $OCH_3$), 2.52 (d, $J$ = 16.2 Hz, 2H, $CH_2$), 2.11 (d, $J$ = 16.2 Hz, 2H, $CH_2$), 1.08 (s, 3H, $CH_3$), 0.97 (s, 3H, $CH_3$). $^{13}$C NMR (75 MHz, DMSO-$d_6$): δ 195.1, 160.7, 158.1, 152.5, 149.8, 142.3, 138.6, 132.3, 129.1, 124.4, 123.3, 117.3, 113.8, 113.5, 111.5, 102.6, 55.3, 50.6, 33.9, 32.6, 29.5, 27.0. Anal. calcd for $C_{25}H_{23}NO_4$: C 74.80, H 5.77, N 3.49; found: 74.76, H 5.73, N 3.52.

### 4.15 | 7-(2,4-Dichlorophenyl)-10,10-dimethyl-7,10,11,12-tetrahydro-6*H*-chromeno[4,3-*b*]quinoline-6,8(9*H*)-dione (4o)

MP: 333–334 °C; (KBr, $\nu$, $cm^{-1}$): 3288, 3071, 2956, 1718, 1689, 1604, 1508, 1475, 1364, 1240, 1198, 1149, 1045, 747. $^1$H NMR (300 MHz, DMSO-$d_6$): δ 9.73 (s, 1H, NH), 8.31 (d, $J$ = 7.5 Hz, 1H, Ar–H), 7.63 (t, $J$ = 7.5 Hz, 1H, Ar–H), 7.28–7.48 (m, 5H, Ar–H), 5.25 (s, 1H, CH), 2.64 (sbr, 2H, $CH_2$), 2.29 (d, $J$ = 16.0 Hz, 1H, $CH_2$), 2.01 (d, $J$ = 16.0 Hz, 1H, $CH_2$), 1.08 (s, 3H, $CH_3$), 0.94 (s, 3H, $CH_3$). $^{13}$C NMR (75 MHz, DMSO-$d_6$): δ 194.9, 160.3, 152.6, 150.6, 143.2, 142.5, 134.0, 133.9, 132.6, 131.7, 128.9, 127.2, 124.5, 123.5, 117.3, 113.1, 110.2, 101.0, 50.5, 34.5, 32.4, 29.5, 26.9. Anal. calcd for $C_{24}H_{19}NO_3Cl_2$: C 65.47, H 4.35, N 3.18; found: 65.50, H 4.36, N 3.22.

### 4.16 | 10,10-Dimethyl-7-(naphthalen-1-yl)-7,10,11,12-tetrahydro-6*H*-chromeno [4,3-*b*]quinoline-6,8(9*H*)-dione (4p)

MP: 322–324 °C; (KBr, $\nu$, $cm^{-1}$): 3309, 3073, 2955, 1724, 1670, 1608, 1574, 1510, 1476, 1361, 1237, 1195, 1147, 1053, 1020, 897, 777. $^1$H NMR (300 MHz, DMSO-$d_6$): δ 9.76 (s, 1H, NH), 8.80 (d, $J$ = 8.7 Hz, 1H, Ar–H), 8.35 (dd, $J$ = 8.1, 1.2 Hz, 1H, Ar–H), 7.81 (dd, $J$ = 8.1, 1.2 Hz, 1H, Ar–H), 7.68 (dd, $J$ = 7.2, 2.4 Hz, 1H, Ar–H), 7.56–7.61 (m, 2H, Ar–H), 7.42–7.51 (m, 2H, Ar–H), 7.31–7.38 (m, 3H, Ar–H), 5.74 (s, 1H, CH), 2.71 (sbr, 2H, $CH_2$), 2.24 (d, $J$ = 16.5 Hz, 1H, $CH_2$), 1.95 (d, $J$ = 16.5 Hz, 1H, $CH_2$), 1.08 (s, 3H, $CH_3$), 0.89 (s, 3H, $CH_3$). $^{13}$C NMR (75 MHz, DMSO-$d_6$): δ 195.1, 160.8, 152.3, 149.5, 145.6, 142.2, 133.2, 131.3, 128.1, 127.2, 127.0, 126.1, 125.8, 125.7, 124.4, 123.4, 117.2, 113.5, 113.0, 103.9, 50.5, 32.5, 30.2, 29.7, 26.7. Anal. calcd for $C_{28}H_{23}NO_3$: C 79.79, H 5.50, N 3.32; found: 80.02, H 5.55, N 3.34.

## ACKNOWLEDGMENTS

Financial support by Rasht Branch, Islamic Azad University is gratefully acknowledged.

## ORCID

*Mahdiye Foroughi Kaldareh* https://orcid.org/0000-0003-3723-6589

*Masoud Mokhtary* https://orcid.org/0000-0003-3763-7139

*Mohammad Nikpassand* https://orcid.org/0000-0002-9692-6849


## REFERENCES


[1] M. Mokhtary, *J. Iran. Chem. Soc.* **2016**, *13*, 1827.

[2] M. Salavati-Niasari, *J. Mol. Catal. A: Chem.* **2004**, *217*, 87.

[3] M. Salavati-Niasari, P. Salemi, F. Davar, *J. Mol. Catal. A: Chem.* **2005**, *238*, 215.

[4] M. Salavati-Niasari, *J. Mol. Catal. A: Chem.* **2005**, *229*, 159.

[5] M. Salavati-Niasari, *J. Mol. Catal. A: Chem.* **2006**, *245*, 192.

[6] M. Salavati-Niasari, *Micropor. Mesopor. Mat.* **2006**, *95*, 248.

[7] M. Salavati-Niasari, *J. Mol. Catal. A: Chem.* **2008**, *283*, 120.

[8] M. Salavati-Niasari, A. Sobhani, *J. Mol. Catal. A: Chem.* **2008**, *285*, 58.

[9] M. Salavati-Niasari, M. Shakouri-Arani, F. Davar, *Micropor. Mesopor. Mat.* **2008**, *116*, 77.

[10] M. Salavati-Niasari, Z. Salimi, M. Bazarganipour, F. Davar, *Inorg. Chim. Acta* **2009**, *362*, 3715.

[11] M. Salavati-Niasari, F. Davar, *Inorg. Chem. Commun.* **2006**, *9*, 263.

[12] S. Zinatloo-Ajabshir, M. Salavati-Niasari, M. Hamadanian, *RSC Adv.* **2015**, *5*, 33792.

[13] S. Zinatloo-Ajabshir, M. Salavati-Niasari, *Compos. Part B.* **2019**, *174*, 106930.

[14] G. Baldi, D. Bonacchi, C. Innocenti, G. Lorenzi, C. Sangregorio, *J. Mag. Magn. Mater.* **2007**, *311*, 10.

[15] Z. Iatridi, K. Vamvakidis, I. Tsougos, K. Vassiou, C. Dendrinou-Samara, G. Bokias, *ACS Appl. Mater. Interfaces* **2016**, *8*, 35059.

[16] H. Gu, K. Xu, Z. Yang, C. K. Chang, B. Xu, *Chem. Commun.* **2005**, *34*, 4270.

[17] A. A. Kudale, J. Kendall, D. O. Miller, J. L. Collins, G. J. Bodwell, *J. Org. Chem.* **2008**, *73*, 8437.

[18] L. D. S. Yadav, S. Singh, V. K. Rai, *Tetrahedron Lett.* **2009**, *50*, 2208.

[19] C. Anderle, S. M. Li, B. Kammerer, B. Gust, L. Heide, *J. Antibiot.* **2007**, *60*, 504.

[20] E. K. Lewis, W. C. Haaland, F. Nguyen, D. A. Heller, M. J. Allen, R. R. MacGregor, C. S. Berger, B. Willingham, L. A. Burns, G. B. Scott, C. Kittrell, B. R. Johnson, R. F. Curl, M. L. Metzker, *Proc. Natl. Acad. Sci. U. S. a.* **2005**, *102*, 5346.

[21] P. R. Kym, R. Iyengar, A. J. Souers, J. K. Lynch, A. S. Judd, J. Gao, J. Freeman, M. Mulhern, G. Zhao, A. Vasudevan, D. Wodka, C. Blackburn, J. Brown, J. L. Che, C. Cullis, S. J. Lai, M. J. LaMarche, T. Marsilje, J. Roses, T. Sells, B. Geddes, E. Govek, M. Patane, D. Fry, B. D. Dayton, S. Brodjian, D. Falls, M. Brune, E. Bush, R. Shapiro, V. Knourek-Segel, T. Fey, C. McDowell, G. A. Reinhart, L. C. Preusser, K. Marsh, L. Hernandez, H. L. Sham, C. A. Collins, *J. Med. Chem.* **2005**, *48*, 5888.

[22] Y. Jacquot, I. Laïos, A. Cleeren, D. Nonclercq, L. Bermont, B. Refouvelet, K. Boubekeur, A. Xicluna, G. Leclercq, G. Laurent, *Bioorg. Med. Chem.* **2007**, *15*, 2269.

[23] T. A. Fattah, A. Saeed, P. A. Channar, F. A. Larik, M. Hassan, H. Raza, Q. Abbas, *S. Y. Seo. Drug Res.* **2018**, *68*, 378.

[24] M. Mohammadi-Khanaposhtani, H. Yahyavi, E. Barzegaric, S. Imanparast, M. M. Heravii, M. A. Faramarzi, A. Foroumadi, H. Adibi, B. Larijani, M. Mahdavi, *Polycycl. Aromat. Comp* **2018**. in press

[25] M. H. Sayahi, S. J. Saghanezhad, M. Mahdavi, *Res. Chem. Intermed.* **2018**, *44*, 739.

[26] Z. Chen, X. Yang, W. Su, *Tetrahedron Lett.* **2015**, *56*, 2476.

[27] Z. Chen, J. Gu, W. Su, *J. Chem. Res.* **2013**, *37*, 327.

[28] S. Mukherjee, S. Sarkar, A. Pramanik, *Chemistry Select* **2018**, *3*, 1537.

[29] M. R. Rezaei, M. Sarvaretaherabadi, *Arab. J. Chem.* **2017**, *10*, S1287.

[30] S. Paul, A. R. Das, *Catal. Sci. Technol.* **2012**, *2*, 1130.

[31] H. Yahyavi, M. M. Heravi, M. Mahdavi, A. Foroumadi, *Tetrahedron Lett.* **2018**, *59*, 94.

[32] S. Paul, A. R. Das, *Tetrahedron Lett.* **2012**, *53*, 2206.

[33] R. Motamedi, G. R. Bardajee, S. Shakeri, *Heterocycl. Commun.* **2014**, *20*, 181.

[34] N. Azgomi, M. Mokhtary, *J. Mol. Catal. A: Chem.* **2015**, *398*, 58.

[35] S. Vajar, M. Mokhtary, *Polycycl. Aromat. Comp.* **2019**, *39*, 111.

[36] V. S. Kumbhar, A. D. Jagadale, N. M. Shinde, C. D. Lokhande, *Appl. Surf. Sci.* **2012**, *39*, 259.

[37] K. Maaz, A. Mumtaz, S. K. Hasanain, A. Ceylan, *J. Magn. Magn. Mater.* **2007**, *289*, 308.

[38] R. Miri, R. Motamedi, M. R. Rezaei, O. Firuzi, A. Javidnia, A. Shafiee, *Arch. Pharm. Chem. Life Sci.* **2011**, *2*, 111.

[39] A. Yahya-Meymandi, H. Nikookar, S. Moghimi, M. Mahdavi, L. Firoozpour, A. Asadipour, P. Rashidi Ranjbar, A. Foroumadi, *J. Iran. Chem. Soc.* **2017**, *14*, 771.



**How to cite this article:** Foroughi Kaldareh M, Mokhtary M, Nikpassand M. Nicotinic acid-supported cobalt ferrite-catalyzed one-pot synthesis of substituted chromeno[3,4-*b*]quinolines. *Appl Organometal Chem*. 2020;e5469. https://doi.org/10.1002/aoc.5469